Reaction Routes Leading to CO_2 and CO in the Briggs−Rauscher Oscillator: Analogies between the Oscillatory BR and BZ Reactions

Norbert Muntean,[†] Gabriella Szabó,[†] Maria Wittmann,*[,‡] Thuy Lawson,[‡] János Fülöp,[‡] Zoltán Noszticzius,[‡] and Lavinia Onel[§]

Department of Physical Chemistry, "Babeş-Bolyai" University, RO-400028 Cluj-Napoca, Romania, Center for Complex and Nonlinear Systems and the Department of Physics, Budapest University of Technology and Economics, H-1521 Budapest, Hungary, and Faculty of Chemistry, "Al.I.Cuza" University, RO-700506 Iaşi, Romania

Received: June 4, 2009

With Fenton-type experiments, it is shown that the intense CO_2/CO evolution in the Briggs−Rauscher (BR) reaction is due to decarboxylation/decarbonylation of organic free radicals. The metal ion applied in the Fenton-type experiments was Fe^{2+} or Ti^{3+} or Mn^{2+} combined with H_2O_2 or $S_2O_8^{2-}$ as a peroxide, whereas the organic substrate was malonic acid (MA) or a 1:1 mixture of MA and iodomalonic acid (IMA). Experiments with a complete BR system applying MA or the MA/IMA mixture indicate that practically all CO_2 and CO comes from IMA. The decarboxylation/decarbonylation mechanisms of various iodomalonyl radicals can be analogous to that of the bromomalonyl radicals studied already in the Belousov−Zhabotinsky (BZ) reaction. It is found that an intense CO_2/CO evolution requires the simultaneous presence of H_2O_2, IO_3^-, Mn^{2+}, and IMA. It is suggested that the critical first step of this complex reaction takes place in the coordination sphere of Mn^{2+}. That first step can initiate a chain reaction where organic and hydroperoxyl radicals are the chain carriers. A chain reaction was already found in a BZ oscillator as well. Therefore, the analogies between the BR and BZ oscillators are due to the fact that in both mechanisms, free radicals and, in most cases, also transition-metal complexes play an important role.

Introduction

The most dramatic oscillating reaction in solution is probably the one discovered by Briggs and Rauscher.[1] If appropriate amounts of acidic iodate, hydrogen peroxide, manganous salt, malonic acid (MA), and starch indicator are mixed in aqueous solution, then the system repeats several times the sequence colorless → yellow → blue → colorless. The frequency is a few cycles per minute, and the transition from yellow to blue is particularly sharp. This is the so-called classical Briggs−Rauscher (BR) oscillator, which is a prime example of nonlinear behavior in chemistry.[2−4]

Since its discovery, the classical BR oscillator and its various modifications applying antioxidant-type inhibitors or new substrates were studied in several laboratories.[5−17] Until now, however, all mechanisms suggested for the classical BR oscillator[5−12] focused on its inorganic subset and omitted the organic subset nearly completely, except the following two reactions that describe the iodination of MA

$$\mathrm{MA} \leftrightarrow \mathrm{MA(enol)} \tag{1}$$

$$\mathrm{I_2 + MA(enol) \rightarrow IMA + I^- + H^+} \tag{2}$$

where MA and MA(enol) denote malonic acid and its enolic form, respectively, and IMA stands for iodomalonic acid. Redox reactions of MA and IMA were not included in these schemes. The only exception was a model by Vukojevic et al.,[10] who suggested the following hypothetical reaction in their model Q (a model based on quenching experiments)

$$\mathrm{2IMA + H_2O_2 \rightarrow I_2 + U} \tag{3}$$

where U denotes "unknown (inactive) products" of the reaction. Formally, eq 3 can be regarded as a reduction of IMA by H_2O_2 if U includes MA. There was no theory or experiment, however, that would suggest that oxidation of the organic substrates can also occur in the BR reaction. Therefore, it was an unexpected discovery when we found intense carbon dioxide and carbon monoxide evolutions in the classical BR reaction.[18] Because these products are not included in the present mechanistic schemes, moreover, they might indicate oxidation of the substrates, we started systematic research to find reaction routes that could lead to these products.

As a first step, in a previous paper,[19] we studied the decarboxylation of diiodomalonic acid, which could be, at least theoretically, an important nonredox source of the CO_2 evolution in the BR reaction according to the following scheme

$$\mathrm{I_2MA \rightarrow I_2AcA + CO_2} \tag{4}$$

where I_2MA and I_2AcA denote diiodomalonic and diiodoacetic acid, respectively. Whereas we found that I_2MA can really decarboxylate with a measurable rate under BR conditions, we could also prove that the contribution of this reaction to the CO_2 production in the BR reaction is negligible.[19]

In this article, we want to test a new hypothesis according to which CO_2 and CO are decomposition (decarboxylation and decarbonylation) products of organic free radicals. These radicals

---

* Corresponding author. E-mail: wittmann@eik.bme.hu.

[†] "Babeş-Bolyai" University.

[‡] Budapest University of Technology and Economics.

[§] "Al.I.Cuza" University.

10.1021/jp905239w CCC: $40.75

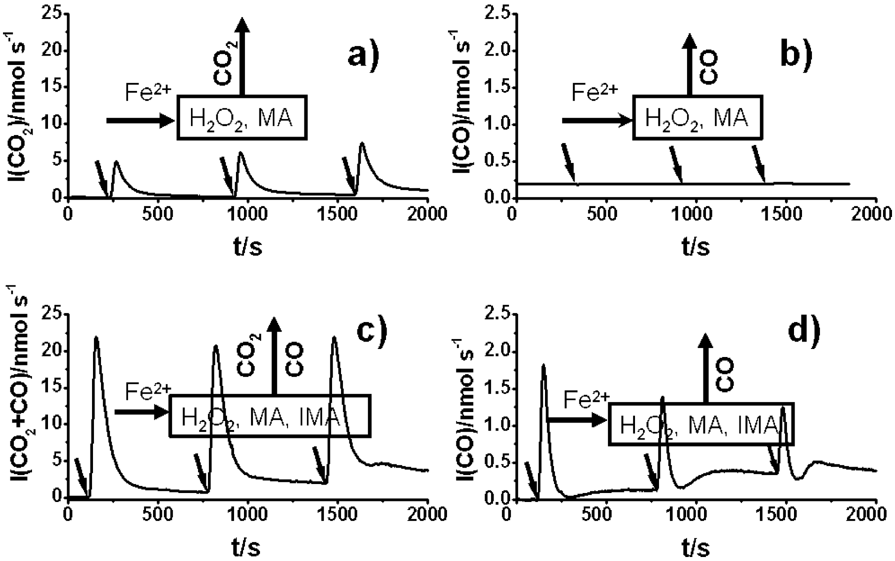

Figure 1. CO_2 and CO evolution from MA or IMA + MA organic substrates in the Fenton reaction of H_2O_2 and Fe^{2+}. Concentrations: $[H_2O_2] = 0.66$ M, $[H_2SO_4] = 25$ mM for parts a−d. Substrate: [MA] = 50 mM for parts a and b, [MA] = [IMA] = 25 mM for parts c and d. Reaction volume: 2 mL. The arrows indicate the start of the reaction when 0.2 M $(NH_4)_2Fe(SO_4)_2$ solution was pumped into the reactor with a flow rate of 200 μL/min for 20 s; that is, altogether, 13.3 μmol Fe^{2+} was injected ($[Fe^{2+}]_0 = 6.4$ mM). The addition of the Fe^{2+} solution was repeated two more times with approximately 10 min intervals. In parts a and c, the CO_2 + CO flow is depicted, whereas, in parts b and d, only the CO flow is depicted.

can be formed when MA and IMA are oxidized by H_2O_2 and IO_3^- in the presence of Mn^{2+} or by inorganic radicals produced in the BR reaction. The inorganic free radicals can be hydroperoxyl ($HOO^•$) or iodine dioxide ($IO_2^•$) radicals, which are proposed intermediates in the various BR mechanisms.[5−12]

The above new hypothesis is also supported by a possible analogy to the Belousov−Zhabotinsky (BZ) reaction. In that reaction, CO_2 and CO evolution were also observed,[20,21] and it was proven[22,23] that the major source of the gas evolution is decarboxylation and decarbonylation of organic radicals, which are formed mostly when bromomalonic acid (a compound analogous to IMA) is oxidized by Ce^{4+} ions[22] and by $BrO_2^•$ radicals.[23]

To prove our hypothesis that CO_2/CO evolution in the BR reaction is due to decarboxylation/decarbonylation of organic free radicals, such radicals were generated in Fenton-type reactions in the presence of MA and IMA organic substrates. The metal ion applied in our Fenton-type experiments was Fe^{2+} or Ti^{3+} or Mn^{2+} combined with H_2O_2 or $S_2O_8^{2-}$ as a peroxide. To compare the observed gas evolution intensities with that of the BR reaction, CO_2 and CO evolution were also measured in a nonoscillatory BR system with MA or MA + IMA substrate, where the Mn^{2+} concentration was the same as that in the Fenton experiments.

Experimental Section

Chemicals. MA (Fluka, puriss.), $NaIO_3$ (Fluka, puriss. p.a.; ≥99.5%), KI (Riedel-deHaën, puriss. p.a.), H_2SO_4 (97%, Merck, p.a.), $(NH_4)_2Fe(SO_4)\cdot 6H_2O$ (Reanal, a.lt.), $TiCl_3$ (Riedel-de-Haën, min. 12%), $MnSO_4\cdot 4H_2O$ (Reanal, a.lt.), H_2O_2 (Fluka, puriss. p.a. ACS; ≥30%) and $Na_2S_2O_8$ (Sigma-Aldrich, purum p.a.) were used as received. All solutions were prepared with doubly distilled water.

Stock Solution S for a 1:1 IMA + MA Substrate Mixture. We prepared the stock solution by applying the method suggested by Noszticzius et al.[24] The 1:1 ratio of [IMA]/[MA] was necessary because pure IMA is unstable toward disproportionation, as was previously shown.[19] First, 6 mL of 1 M MA, 1.2 mL of 5 M H_2SO_4, and 5 mL of 0.2 M $NaIO_3$ were mixed in a 25 mL beaker. Then, 5 mL of 0.4 M KI solution was added dropwise from a buret into the solution under continuous stirring. After each drop of the KI solution, we waited several seconds until the brown color of iodine disappeared. As a result, a 1:1 mixture of MA and IMA was obtained, which is referred to as stock solution "S" in the following. In solution S, the concentration of MA, IMA, and H_2SO_4 is 174 mM. (Beside these components, the mixture also contains sodium and potassium hydrogen sulfate in the same total concentration $[NaHSO_4] + [KHSO_4] = 174$ mM.) Solution S was freshly prepared each day and kept in the refrigerator if not immediately used.

Substrate−Peroxide Mixtures for Fenton-Type Reactions with H_2O_2. In this case, the initial concentration of H_2O_2 was 0.66 M in the reactor, as in our previous BR experiments.[18,19] Other initial concentrations in the reactor were: substrate: 50 mM MA or 25 mM MA + 25 mM IMA, and $[H_2SO_4] = 25$ mM. These solutions were prepared in the following way: (i) When the substrate was pure MA, 1.25 mL of a solution containing 0.2 M MA and 0.1 M H_2SO_4 was mixed in a 5 mL volumetric flask with 1.25 mL of 2.64 M H_2O_2. Then, the volumetric flask was filled up to 5 mL with distilled water. 2 mL of this mixture was used in the semibatch reactor for one experiment. (ii) When the substrate was a mixture of MA and IMA, 1.43 mL of solution S and 2.5 mL of 2.64 M H_2O_2 were mixed in a 10 mL volumetric flask. The flask was filled up with distilled water, and 2 mL of this mixture was used in one experiment.

Substrate−Peroxide Mixtures for Fenton-Type Reactions with $Na_2S_2O_8$. In this case, the initial concentration of $Na_2S_2O_8$ was 0.1 M in the reactor. The substrate and the sulfuric acid concentrations were the same as those in the previous experiments with H_2O_2. The recipes also applied the same reagent concentrations and volumes, except a 0.4 M $Na_2S_2O_8$ stock solution was applied instead of the H_2O_2 solution.

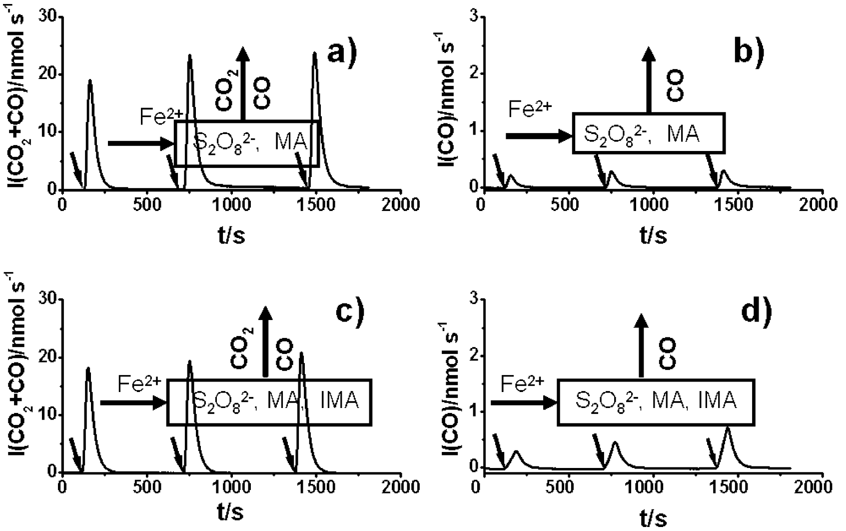

Figure 2. CO_2 and CO evolution from MA or IMA + MA organic substrates in the Fenton-type reaction of $Na_2S_2O_8$ and Fe^{2+}. Concentrations: $[Na_2S_2O_8] = 0.1$ M, $[H_2SO_4] = 25$ mM for parts a−d. Substrate: [MA] = 50 mM for parts a and b, [MA] = [IMA] = 25 mM for parts c and d. Reaction volume: 2 mL. To start the reaction, in the case of parts a and b, the same procedure and the same amount of Fe^{2+} ion was applied like in Figure 1. In experiments depicted in parts c and d, however, 0.02 M $(NH_4)_2Fe(SO_4)_2$ solution was pumped into the reactor with a flow rate of 200 μL/min for 20 s; that is, altogether, 1.33 μmol Fe^{2+} (10 times less than that in parts a and b) was injected ($[Fe^{2+}]_0 = 0.64$ mM). In parts a and c, the CO_2 + CO flow is depicted, whereas in parts b and d, only the CO flow is depicted.

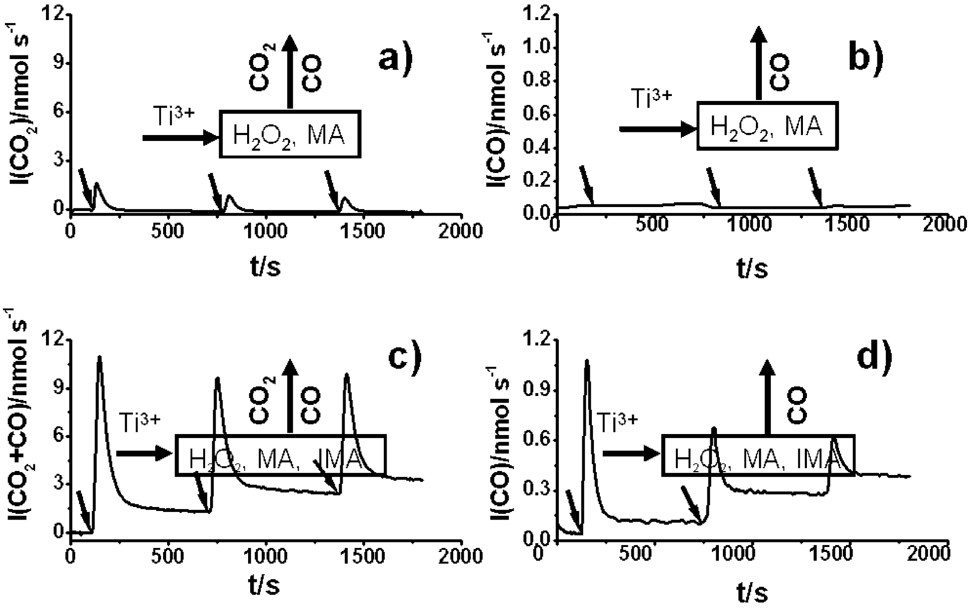

Figure 3. CO_2 and CO evolution from MA or IMA + MA organic substrates in the Fenton-type reaction of H_2O_2 and Ti^{3+}. Concentrations: $[H_2O_2] = 0.66$ M, $[H_2SO_4] = 25$ mM for parts a−d. Substrate: [MA] = 50 mM for parts a and b, [MA] = [IMA] = 25 mM for parts c and d. Reaction volume: 2 mL. To start the reaction, 0.2 M $TiCl_3$ solution was pumped into the reactor with a flow rate of 200 μL/min for 20 s; that is, altogether, 13.3 μmol Ti^{3+} was injected ($[Ti^{3+}]_0 = 6.4$ mM). In parts a and c, the CO_2 + CO flow is depicted, whereas in parts b and d only the CO flow is depicted.

Metal Ion Solutions Applied in the Fenton-Type Reactions. The following metal ion solutions were pumped into the reactor to initiate a Fenton-type reaction: In Figures 1 and 2, an acidic solution of Fe^{2+} was used, where $[(NH_4)_2Fe(SO_4)_2] = 0.2$ and 0.02 M, respectively. In Figures 3 and 4, an acidic solution of Ti^{3+} was used, where $[TiCl_3] = 0.2$ M and 8 mM, respectively, whereas in Figures 5 and 6, an acidic solution of Mn^{2+} was used, where $[MnSO_4] = 0.2$ and 0.02 M, respectively. The acid concentration in the metal ion solutions was $[H_2SO_4] = 25$ mM in all cases.

Fenton-Type Reactions in a Semibatch Reactor. The same semibatch reactor as that previously[19,23] thermostatted to 20 °C was applied. Initially, the reactor was filled with 2 mL of aqueous solution containing the organic substrate (MA or a 1:1 mixture of MA and IMA) and the peroxide (H_2O_2 or $Na_2S_2O_8$). The reaction was initiated by pumping 66 μL of the metal ion (Fe^{2+}, Ti^{3+}, or Mn^{2+}) solution into the reactor by a peristaltic pump applying a flow rate of 200 μL/min for 20 s. Some of the organic free radicals produced in these Fenton-like reactions decarboxylate and decarbonylate and CO_2 and CO were measured. All experiments were repeated three times successively to check whether the products of the Fenton-type reaction affected the CO_2 and CO yield in the consecutive experiments.

Apparatus and Method for CO_2 and CO Measurements. The CO_2 and CO evolution rates were measured by the same instrument, as in our previous publications.[18,19,23] In brief, CO_2 and CO were stripped from the reaction mixture by a N_2 gas flow and were mixed with H_2. Then, CO_2 and CO were

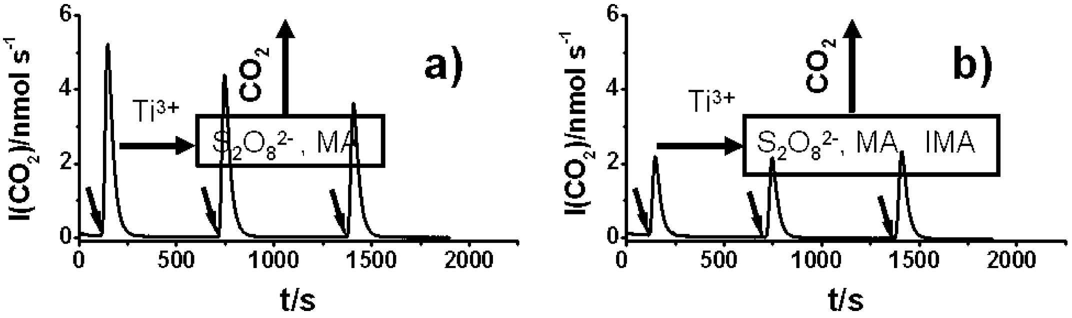

Figure 4. CO_2 evolution from MA or IMA + MA organic substrates in the Fenton-type reaction of $Na_2S_2O_8$ and Ti^{3+}. Concentrations: $[Na_2S_2O_8] = 0.1$ M, $[H_2SO_4] = 25$ mM for parts a and b. Substrate: $[MA] = 50$ mM for part a, $[MA] = [IMA] = 25$ mM for part b. Reaction volume: 2 mL. To start the reaction, 8 mM $TiCl_3$ solution was pumped into the reactor with a flow rate of 200 μL/min for 20 s; that is, altogether, 0.53 μmol Ti^{3+} was injected ($[Ti^{3+}]_0 = 0.26$ mM). In parts a and b, only the CO_2 flow is depicted because CO evolution is below the detection limit.

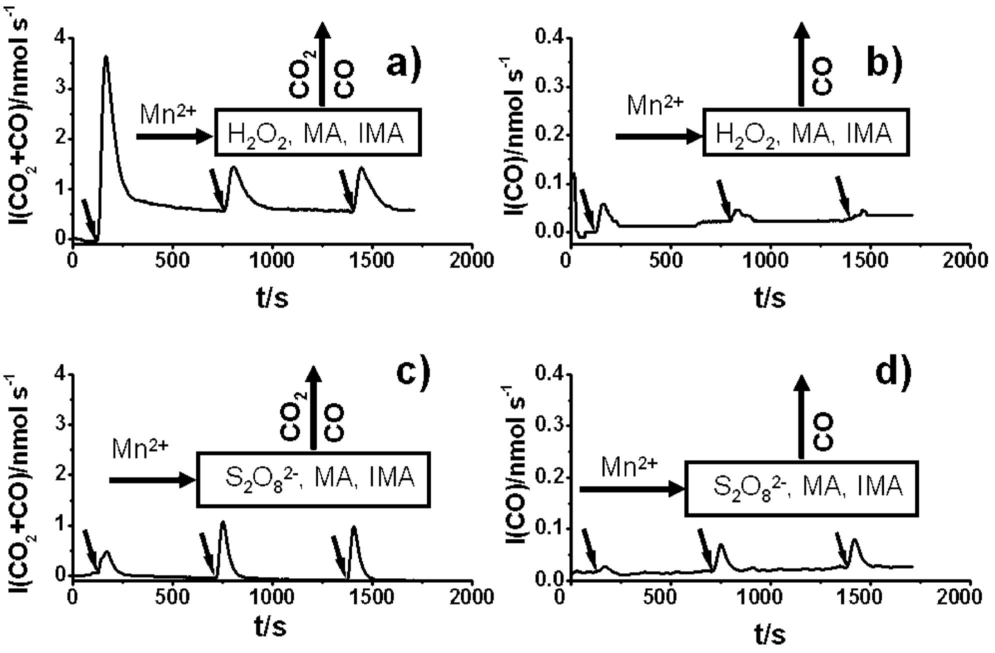

Figure 5. CO_2 and CO evolution from IMA + MA organic substrates in the Fenton-type reaction of Mn^{2+} and H_2O_2 or $Na_2S_2O_8$, respectively. Concentrations: $[MA] = [IMA] = 25$ mM, $[H_2SO_4] = 25$ mM for parts a–d; $[H_2O_2] = 0.66$ M for parts a and b, $[Na_2S_2O_8] = 0.1$ M for parts c and d. Reaction volume: 2 mL. To start the reaction, 0.2 M $MnSO_4$ solution was pumped into the reactor with a flow rate of 200 μL/min for 20 s; that is, altogether, 13.3 μmol Mn^{2+} was injected ($[Mn^{2+}]_0 = 6.4$ mM). In parts a and c, the CO_2 + CO flow is depicted, whereas in parts b and d, only the CO flow is depicted.

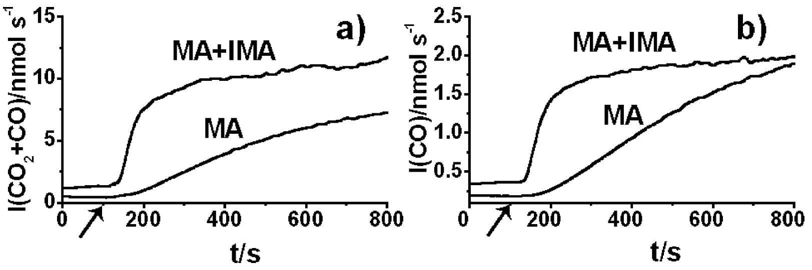

Figure 6. Nonoscillatory BR reaction with a lower-than-usual Mn^{2+} ($[Mn^{2+}]_0 = 0.64$ mM) concentration. The reaction was started by pumping 0.02 M $MnSO_4$ solution for 20 s with a flow rate of 200 μL/min. The start time is indicated by an arrow. Other concentrations: $[H_2O_2] = 0.66$ M, $[NaIO_3] = 0.04$ M, $[H_2SO_4] = 25$ mM, substrate: $[MA] = 50$ mM, or $[MA] = [IMA] = 25$ mM. In part a, the CO_2 + CO flow is depicted, whereas in part b, only the CO flow is depicted.

converted to methane in a catalytic reactor, and the produced CH_4 was measured by a flame ionization detector (FID). A CO_2 or CO injection caused a FID current pulse after a 30 s delay at the applied gas flow rates. Arrows indicating the injection time in the Figures point to times corrected with that time delay (e.g., an arrow points to 130 s if the injection is made at 100 s). Other details of our CO_2/CO measuring apparatus and method can be found in ref 23. N_2 and H_2 flow rates were 40 mL/min in the present experiments.

Results and Discussion

According to our working hypothesis, CO_2 and CO produced in the BR reaction are decarboxylation and decarbonylation products of organic free radicals. Presently, it is not yet known how these radicals are formed. One possibility would be that they appear when MA, IMA, or both react with some inorganic free radical intermediates of the BR reaction. In the current BR theories, there are two inorganic radicals in the mechanism, namely, the hydroperoxyl radical, $^{\bullet}OOH$ (which is a protonated superoxide radical), and the iodine dioxide radical, $^{\bullet}OIO$. Unfortunately, no method is known for a selective production of these radicals; therefore, we decided to generate radicals by Fenton-type reactions.

As can be seen in our experiments, the way that organic radicals were generated is different from the way they are formed in the BR system. It is reasonable to assume, however, that the organic radicals formed in the Fenton-type reactions are qualitatively the same independently of the inorganic oxidant. This is because when the inorganic oxidant removes an electron from the organic molecule, a mixture of various organic radicals is produced (because the electron can be removed from different parts of the organic substrate), but the components of this mixture are probably the same independently of the chemical character of the oxidizing agent. Naturally, the relative amount of the different organic radicals may depend on the given Fenton-type reagent. Nevertheless, we can hope that those radicals that are able to decarboxylate and decarbonylate in the BR reaction will also appear when MA or IMA is oxidized in Fenton-type systems. Therefore, to prove our hypothesis, we applied different Fenton-type reagents together with MA or IMA while we recorded CO_2 and CO evolution.

Generating Organic Radicals with Fenton-Type Reagents. The classical Fenton reagent refers to a reacting mixture of hydrogen peroxide and the aqueous solution of a ferrous salt. Besides this reagent, however, in our experiments, we applied some analogous systems as well. The analogous Fenton-type reagents are mixtures of peroxides (R′OOR″) with metal complexes (L_mM^n) in their low-valent oxidation states. (In our experiments, the ligand L was water.) Fenton-like reactions play an important role in a variety of catalytic and biological processes. We can generalize these reactions by the following equation[25]

$$R'OOR'' + L_mM^n \rightarrow {}^{\bullet}OR' + OR''^{-} + L_mM^{n+1}$$

where R′ and R″ can be different. Detailed kinetic studies and thermodynamic considerations indicate that in most cases $^{\bullet}OR'$ radicals (e.g., hydroxyl radicals) are not formed in these reactions. In the case of H_2O_2, for example, the detailed mechanism seems to involve the formation of a transition-metal peroxide complex via inner sphere mechanism[25]

$$H_2O_2 + L_mM^n \leftrightarrow L_mM^n{\cdot}H_2O_2 \quad \text{or} \quad L_{m-1}M^n{\cdot}H_2O_2 + L$$

followed by one of the ensuing routes (RH: organic substrate)

$$L_{m-1}M^n{\cdot}H_2O_2 + L \rightarrow L_mM^{n+1} + {}^{\bullet}OH + OH^-$$

$$L_{m-1}M^n{\cdot}H_2O_2 \rightarrow L_{m-1}M^{n+2} = O + H_2O$$

$$L_{m-1}M^n{\cdot}H_2O_2 + L + RH \rightarrow L_mM^{n+1} + R^{\bullet} + H_2O + OH^-$$

$$^{\bullet}OH + RH \rightarrow R^{\bullet} + H_2O$$

$$L_{m-1}M^{n+2} = O + RH + L \rightarrow L_mM^{n+1} + R^{\bullet} + OH^-$$

According to the above schemes, either the hydroxyl radical reacts with the organic substrate RH forming an organic radical $R^{\bullet}$, or the organic substrate is directly oxidized by $L_{m-1}M^n{\cdot}H_2O_2$ or by $L_{m-1}M^{n+2} = O$. In any case, the first oxidation product of the organic substrate RH is the organic radical $R^{\bullet}$ (which can be a mixture of various radicals, however, as we have mentioned earlier). Therefore, without having any exact information about the chemical nature of the direct oxidant (whether it is an inorganic free radical or a metal complex of the peroxide) we can be rather sure that the first oxidation products of MA and IMA are organic free radicals.

CO_2 and CO Yield from MA and from IMA Substrates Applying Various Fenton-Type Systems. Obviously, the CO_2 and CO yields obtained with the different Fenton systems can be different, even if the organic substrate is the same. In the present research, however, the most important aim is not to compare the CO_2 and CO yields of the different Fenton systems for the same substrate but to compare that yield for different substrates. This can be helpful in deciding whether the source of CO_2 and CO in the BR reaction is MA or IMA.

In the series of Figures 1−5, the rate of CO_2 and CO evolution is shown when applying different peroxides and different metals as Fenton reagents to generate radicals. In each Figure, the two substrates, MA (a and b) and IMA (c and d) are compared. Because of its instability, IMA was mixed with an equal amount of MA so that the total substrate concentration was always the same. The concentrations of all species were chosen to be similar to the BR conditions. However, in some cases, the metal ion concentration was decreased to downsize the CO_2 peak. In Figures a and c, the sum of the CO_2 and CO currents are shown, whereas on b and d, only the CO currents are shown. In some cases, the CO current is negligible compared with the CO_2 current, so parts a and c can be considered to be CO_2 currents. The applied substrate, peroxide, and metal and the measured gas are indicated on each Figure.

In Figure 1 radicals are generated with the classical Fenton system by the reaction of Fe^{2+} and H_2O_2. It can be seen that the CO_2 + CO evolution rate is about five times higher when the substrate is IMA + MA. CO can be detected only with IMA as the substrate; its quantity is about 5% of the evolved gas. (Note that the scale is one tenth for CO.) The radical generating process was repeated two more times to check whether the products of the Fenton reaction have an effect on the reaction or not. It can be observed that after the peaks the baseline is higher; that is, there remains a small steady flow of CO_2 and CO. This indicates that some radical generating process still goes on when all added Fe^{2+} ions are oxidized to Fe^{3+} ions. Furthermore, the ensuing peaks are different in height; the tendency is to increase with the MA substrate and to decrease with the IMA substrate. The change in the subsequent peaks is not so dramatic, however, and thus it is reasonable to assume that the reaction products do not play an important role in the gas production.

TABLE 1: Percent Yield of CO_2 and CO in Various Fenton-Type Reactions[a]

metal	peroxide	substrate	CO_2 yield %	CO yield %	figure no.
Fe^{2+}	H_2O_2	MA	3.26		1a,b
		IMA + MA	15.2	0.71	1c,d
	$Na_2S_2O_8$	MA	7.82	0.085	2a,b
		IMA + MA	76.6	1.47	2c,d
Ti^{3+}	H_2O_2	MA	0.55		3a,b
		IMA + MA	6.88	0.49	3c,d
	$Na_2S_2O_8$	MA	48.2		4a
		IMA + MA	20.8		4b
Mn^{2+}	H_2O_2	MA			
		IMA + MA	2.68	0.03	5a,b
	$Na_2S_2O_8$	MA			
		IMA + MA	0.22	0.019	5c,d

[a] Percent yield is the ratio of the number of gas molecules (CO_2 or CO) produced in the given Fenton-type reaction compared with the number of metal ions injected into the reactor. (Therefore, for example, the percent CO_2 yield is 100% if one injected metal ion generates one CO_2 molecule.) The CO_2 or CO yield is calculated always from the integral of the first peak.

In Figure 2, the applied metal is again Fe^{2+}, but H_2O_2 is replaced by $Na_2S_2O_8$. Here the quantity of the evolved gas increases by more than one order of magnitude compared with $Fe^{2+} + H_2O_2$ in the case of IMA + MA substrate (Figure 2c,d), so the concentration of Fe^{2+} was decreased to one tenth of the former to obtain about the same peak heights. In the case of MA substrate (Figure 2a,b), the same Fe^{2+} concentration was applied as that with H_2O_2. This is the only Fenton-like reaction where a measurable amount of CO is produced from pure MA substrate. With IMA + MA, about 10 times more CO_2 and 20 times more CO is produced than with MA. The repeated addition of Fe^{2+} shows that the baseline does not increase after the peak in these experiments, but the subsequent peak heights increase slightly.

In Figure 3, Ti^{3+} is used with H_2O_2. Again, there is no CO coming from MA, but the quantity of CO_2 is also much smaller than that in Figure 1, where Fe^{2+} was used. The successive peaks are always smaller than the former ones; the baseline increases greatly after the peaks when IMA is the substrate.

In Figure 4, Ti^{3+} is combined with $Na_2S_2O_8$. Here the Ti^{3+} concentration was much smaller than that before because in experiments with the usual concentration (not shown here), the subsequent peak heights decreased dramatically (each peak was about one-third of the previous one). The most interesting observation is that here MA gives about two times more CO_2 than IMA + MA, whereas in all other cases, the situation is the opposite; IMA + MA usually gives much more CO_2. CO evolution is also below the detection limit with IMA as substrate, so it is not depicted in Figure 4. The baseline always goes back to the original level.

In Figure 5, the applied metal is Mn^{2+}, the catalyst of the BR reaction. In this case, no gas evolution could be detected at all when the substrate was MA alone, and thus those experiments are not shown here. Even with IMA, the total amount of the evolved CO_2 + CO is by far the smallest with this metal. The ratio of the evolved CO compared with CO_2 is about 1% with H_2O_2 and about 10% with $Na_2S_2O_8$. When Mn^{2+} is applied with H_2O_2, there is a characteristic baseline increase after the first peak.

Quantitative data about CO_2 and CO evolution from MA or IMA + MA in the Fenton-type reactions with the different metals and peroxides can be found in Table 1. Note that in most cases, the amount of the evolved CO_2 is at most 20%, but MA gives 48.2% CO_2 with $Ti^{3+} + Na_2S_2O_8$ and IMA + MA gives 76.6% CO_2 with $Fe^{2+} + Na_2S_2O_8$.

In Figure 6, all components of the BR reaction are put together, but the Mn^{2+} concentration is smaller. This way the gas evolution is also smaller than that in the BR (which would be out of scale), and no oscillations appear.

Conclusions

(1) The intense CO_2 and CO evolution observed in the BR reaction is due to decarboxylation and decarbonylation of organic free radicals formed in the reaction. This conclusion is supported by experiments where the organic free radicals were generated in various Fenton-like systems applying MA and IMA as organic substrates. As Figures 1−5 show, these Fenton-like reactions are always followed by CO_2 and often by CO evolution (except for the Mn^{2+}−MA combination, see more in the next paragraph), indicating decarboxylation/decarbonylation of the organic free radicals formed in the reaction.

(2) In all Fenton experiments (except in Figure 4, where the applied metal ion was Ti^{3+} combined with $S_2O_8^{2-}$ as a peroxide) IMA produced more (sometimes several times more) CO_2 and CO than MA. In particular, when Mn^{2+} was used with pure MA, the amount of the evolved gas was so small that it was below the detection limit.

More importantly, when all BR components were put together and the reaction was started by the injection of Mn^{2+} in a smaller-than-usual concentration (Figure 6), an intense CO_2 + CO evolution started immediately if IMA was present, but the initial gas evolution was weak if the substrate was pure MA. Therefore, it is reasonable to conclude that in the oscillatory BR reaction the source of the CO_2 and the CO evolution is IMA. (More precisely, the organic free radicals formed from IMA.)

In this respect, it is important to mention that Furrow discovered CO_2 evolution in a BR reaction with methylmalonic acid.[26] It would be interesting to check whether in that case CO evolution also occurs, and the role of iodo-methylmalonic acid is analogous to that of IMA in the classical BR oscillator.

(3) Fenton-like experiments with Mn^{2+} and MA + IMA as organic substrate (Figure 5) produced very small CO_2 and CO quantities compared with other Fenton experiments (Figures 1−4) or compared with a nonoscillatory BR system where IO_3^- was also present (Figure 6). Our preliminary experiments have shown, however, that acidic IO_3^- alone without H_2O_2 is also not enough to provoke a gas evolution: when Mn^{2+} was injected into a reactor containing acidic IO_3^-, MA, and IMA in the usual concentrations, no measurable CO_2 or CO evolution was observed. Therefore, an intense gas evolution requires the simultaneous presence of Mn^{2+}, H_2O_2, IMA, and IO_3^- in an acidic medium. If any of these components is missing, then only very weak or no gas evolution is possible.

(4) It is interesting to observe that in some cases an increase in the baseline appears after the peak. This never happens when the peroxide is $Na_2S_2O_8$ and always occurs when the peroxide is H_2O_2 and IMA + MA is the substrate. This indicates a catalytic Haber−Weiss-type[27] cycle including also the slow reduction of the high-valent metal ion M^{n+1}, which can produce hydroperoxyl radicals

$$M^{n+1} + H_2O_2 \rightarrow M^n + H^+ + HOO^{\bullet}$$

and these inorganic radicals can react with the organic substrate, producing this way organic radicals and finally CO_2 and CO.

(5) All Fenton-type reactions gave characteristically different CO_2 and CO amounts depending on the metal ion, the peroxide, and the organic substrate applied in the experiment. Obviously, each Fenton-type reaction has a more or less individual mechanism; only their ability to produce organic free radicals is common.

Open Problems and Hypotheses

(1) To explain in detail why all BR components + IMA are needed for an intense CO_2 + CO evolution requires further research. A possible qualitative scheme, however, can already be suggested now on the basis of our experiments and present BR theories.[5−12] In these mechanisms, a temporary oxidation of Mn^{2+} by acidic iodate is assumed, followed by its rapid reduction by H_2O_2. In the FCA model,[14,28] this complex process is lumped into a single step

$$\mathrm{HOIO} + 2\mathrm{H_2O_2} + \mathrm{Mn(II)} \rightarrow 2\mathrm{HOO}^{\bullet} + \mathrm{HOI} + \mathrm{Mn(II)} + \mathrm{H_2O} \quad (5)$$

(The iodous acid HOIO is coming from the iodate−iodide reaction.) The hydroperoxyl radicals formed in the above process can react with IMA to produce various organic radicals that can decarboxylate/decarbonylate. A decarboxylated or decarbonylated organic radical might further react with H_2O_2, and in this route, a new hydroperoxyl radical can appear. This chain mechanism can greatly amplify the gas evolution if the chain is long. We remark that such a chain mechanism associated with CO_2 evolution was already observed in a bromate oscillator.[29]

(2) CO_2 and CO yields in various Fenton-like systems with the same organic substrate vary widely depending on the applied metal ion and the peroxide. It is difficult to explain such a diverse behavior if we assume that the same inorganic radical is formed as a first intermediate when a given peroxide oxidizes different metal ions. Because the total amount of the inorganic free radical generated by a metal ion would depend mostly on the amount of the injected metal ion, the amount of CO_2 + CO should be comparable for different metal ions. But this is clearly not the case.

A reasonable explanation for the observed diversity is that free inorganic radicals are not formed in the Fenton-like systems studied here but the reaction leading to the organic free radicals takes place within the coordination sphere of the metal ion. For example, in the case of Fe^{2+}, as a lower-valent metal ion, and H_2O_2, as a peroxide in acidic medium, they form an $Fe(OH)^{3+}$ ion (with further five coordinated water molecules in the ligand sphere)[30] and this four-valent complexed iron is the actual oxidizing agent. It is also reasonable to assume that the organic substrate may enter into the inner sphere before the reaction. This is a reasonable assumption because MA can form inner sphere chelate complexes with iron ions.[31]

The difference between the properties of the various complexes can explain the wide differences measured in the CO_2 and CO yields. Such an explanation is also in agreement with the present theories of the Fenton-like reactions and also with coordination chemistry.[25,32] Because many BZ oscillators are also catalyzed by transition-metal ions and their complexes, analogous organic radical-forming reactions can also occur in their coordination sphere.

(3) Decarboxylation and decarbonylation of malonyl and bromomalonyl radicals were already studied in the BZ reaction.[23] We suggest that in the course of the classical BR oscillator (organic substrate: MA), first IMA and then iodomalonyl radicals are formed, which decarboxylate and decarbonylate in a way analogous to that of bromomalonyl radicals.

Acknowledgment. This work was partially supported by OTKA grants K-60867 and K-77908 and by the foundation Domus Hungarica Scientiarum et Artium. N.M. and L.O. thank the ESF Programme Functional Dynamics for supporting their visits. We thank Stanley D. Furrow for helpful advice and suggestions.

References and Notes

(1) Briggs, T. S.; Rauscher, W. C. *J. Chem. Educ.* **1973**, *50*, 496.
(2) *Oscillations and Traveling Waves in Chemical Systems*; Field, R. J., Burger, M., Eds.; Wiley: New York, 1985.
(3) Gray, P.; Scott, S. *Chemical Oscillations and Instabilities. Nonlinear Chemical Kinetics*; Clarendon: Oxford, U.K., 1994.
(4) Epstein, I. R.; Pojman, J. A. *An Introduction to Nonlinear Chemical Dynamics*. Oxford University Press: New York, 1998.
(5) Furrow, S. D.; Noyes, R. M. *J. Am. Chem. Soc.* **1982**, *104*, 38.
(6) Furrow, S. D.; Noyes, R. M. *J. Am. Chem. Soc.* **1982**, *104*, 42.
(7) Noyes, R.; Furrow, S. D. *J. Am. Chem. Soc.* **1982**, *104*, 45.
(8) De Kepper, P.; Epstein, I. R. *J. Am. Chem. Soc.* **1982**, *104*, 49.
(9) Turányi, T. *React. Kinet. Catal. Lett.* **1991**, *45*, 235.
(10) Vukojevic, V.; Sørensen, P. G.; Hynne, F. J. *J. Phys. Chem.* **1996**, *100*, 17175.
(11) Kim, K. R.; Lee, D. J.; Shin, K. J. *J. Chem. Phys.* **2002**, *117*, 2710.
(12) Kim, K. R.; Shin, K. J.; Lee, D. J. *J. Chem. Phys.* **2004**, *121*, 2664.
(13) Cervellati, R.; Höner, K.; Furrow, S. D.; Neddens, C.; Costa, S. *Helv. Chim. Acta* **2001**, *84*, 3533.
(14) Furrow, S. D.; Cervellati, R.; Amadori, G. *J. Phys. Chem. A* **2002**, *106*, 5841.
(15) Cervellati, R.; Höner, K.; Furrow, S. D.; Mazzanti, F.; Costa, S. *Helv. Chim. Acta* **2004**, *87*, 133.
(16) Furrow, S. D.; Höner, K.; Cervellati, R. *Helv. Chim. Acta* **2004**, *87*, 735.
(17) Cervellati, R.; Furrow, S. D. *Inorg. Chim. Acta* **2007**, *360*, 842.
(18) Szabó, G.; Csavdári, A.; Onel, L.; Bourceanu, G.; Noszticzius, Z.; Wittmann, M. *J. Phys. Chem. A* **2007**, *111*, 610.
(19) Onel, L.; Bourceanu, G.; Wittmann, M.; Noszticzius, Z.; Szabó, G. *J. Phys. Chem. A* **2008**, *112*, 11649.
(20) Degn, H. *Nature* **1967**, *213*, 589.
(21) Noszticzius, Z. *J. Phys. Chem.* **1977**, *81*, 185.
(22) Nagygyőry, Sz.; Wittmann, M.; Pintér, Sz.; Visegrády, A.; Dancsŏ, A.; Nguyen, B. T.; Noszticzius, Z.; Hegedűs, L.; Försterling, H.-D. *J. Phys. Chem. A* **1999**, *103*, 4885.
(23) Onel, L.; Wittmann, M.; Pelle, K.; Noszticzius, Z.; Sciascia, L. *J. Phys. Chem. A* **2007**, *111*, 7805.
(24) Noszticzius, Z.; Ouyang, Q.; McCormick, W. D.; Swinney, H. L. *J. Am. Chem. Soc.* **1992**, *114*, 4290.
(25) Masarwa, A.; Rachmilovich-Calis, S.; Meyerstein, N.; Meyerstein, D. *Coord. Chem. Rev.* **2005**, *249*, 1937.
(26) Furrow, S. D. *J. Phys. Chem.* **1981**, *85*, 2026–2031.
(27) Walling, C.; Goosen, A. *J. Am. Chem. Soc.* **1973**, *95*, 2987.
(28) Keresztúri, K.; Szalai, I. *Z. Phys. Chem.* **2006**, *220*, 1071.
(29) Pelle, K.; Wittmann, M.; Lovrics, K.; Noszticzius, Z. *J. Phys. Chem. A* **2004**, *108*, 7554.
(30) Kremer, M. L. *J. Phys. Chem. A* **2003**, *107*, 1734.
(31) Deneux, M.; Meilleur, R.; Benoit, R. L. *Can. J. Chem.* **1968**, *46*, 1383.
(32) Goldstein, S.; Meyerstein, D. *Acc. Chem. Res.* **1999**, *32*, 547.

JP905239W